



Application of hydroxy-aluminum- and cetyltrimethylammonium bromide-intercalated bentonite for removing acid and reactive dyes

Faiza Zahaf^a, Nacer Dali^a, Reda Marouf^{a,*}, Fatima Ouadjenia^a, Jacques Schott^b

^aLaboratory of Materials, Applications and Environment, Mustapha Stambouli University, B.P 763 Mamounia road, Mascara 29000, Algeria, emails: zahaf.faiza@yahoo.fr (F. Zahaf), n_dali29@yahoo.fr (N. Dali),

Tel./Fax: +213 45 81 39 98; emails: reda_marouf@hotmail.com (R. Marouf), fatouadj2@yahoo.fr (F. Ouadjenia)

^bLaboratoire Géosciences Environnement Toulouse, CNRS (UMR 5563)-OMP-Université Paul-Sabatier, Toulouse, France, email: jaques.schott@get.obs-mip.fr

Received 1 June 2015; Accepted 14 October 2015

ABSTRACT

In this study, modified pillared montmorillonites were prepared using hydroxy-aluminum and cetyltrimethylammonium bromide by the intercalation method and applied as adsorbents to remove acid and reactive dyes from aqueous solutions. The dyes used in this work are Bemacid Yellow E-4G and Procion Yellow MX-4R. The main compositions of raw and pillared bentonite were characterized by chemical composition, X-ray diffraction, and BET specific surface area. The removal efficiency of dyes was studied as a function of pH, initial dye concentrations, and contact time. The removal efficiency of two dyes by cetyltrimethylammonium bromide-intercalated bentonite was more than that of hydroxy-aluminum in similar conditions. The results showed that the maximum adsorption of modified bentonite was obtained at a range of pH 2–3. The maximum adsorption capacity was estimated to be 94 mg/g at room temperature. The study of the adsorption kinetic model revealed that the pseudo-second-order model was the best applicable one to describe the adsorption of dyes onto pillared bentonites. Adsorption data were analyzed by both Langmuir and Freundlich adsorption isotherms, and the results showed that it was better described by the Freundlich model.

Keywords: Bentonite; Cethyltrimethylammonium bromide; Hydroxy-aluminum; Dyes; Adsorption isotherm

1. Introduction

The bentonite is a clay material which contains essentially the montmorillonite (Mt). This clay mineral is evolved from volcanic ashes by weathering or hydrothermal effects and is a 2:1 type of aluminosilicates. Each 2:1 layer of Mt has two silica tetrahedral

sheets bonded to a central alumina octahedral sheet [1,2].

Generally, the bentonites are widely used in many industrial applications such as drilling, foundry, ceramics, paint, pharmaceuticals, cement, and paper industries [3–6]. They can also be used as an adsorbent to remove various organic or inorganic pollutants in the aqueous solution [7,8]. Despite significant physicochemical properties that have this type of clay,

*Corresponding author.

they can be substantially improved by a structural change inserting of the pillars such as hydroxyaluminum cations [9,10] or organic compounds as alkyl ammonium [11]. The pillaring of the clay lies in the intercalation of chemical species between the sheets in order to obtain microporous materials with rigid structure and a large interlayer spacing [12].

Polyhydroxy aluminum cation intercalation in clay consists in the insertion between the layers of "Al₁₃" referred to as Keggin molecule, [AlO₄Al₁₂(OH)₂₄(H₂O)₁₂] [13]. The presence of surface negative charge and large amount of exchangeable positive ions result in the cover of a layer of water molecule on the mineral surface, which makes natural bentonite exhibit strong hydrophilicity, and therefore, it is not an effective adsorbent for organic pollutants. The occupation of exchange sites on the bentonite surface by ammonium surfactants cations such as cethyltrimethylammonium will change the surface properties from hydrophilic to hydrophobic [14]. Therefore, there has been much interest in the use of modified bentonites as adsorbents to prevent and remediate environmental organic contamination.

Recently, the synthetic dyes are consumed broadly in textile industries, and large volumes of dye wastewater are produced. It is estimated that about 10,000 t are discharged annually and around 50% of all dyes are azo dyes (–N=N–) [15]. To these environmental contaminants, modified clay minerals are good candidate adsorbents for the treatment of dyes from wastewaters due to their exclusive features, such as abundance, low cost materials, high specific surface areas, inexpensive availability, environmental stability, and high adsorptive and ion exchange properties [16,17].

The aim of the present work was to investigate and compare the efficiency of two adsorbents toward the adsorption of acid Yellow E-4G and reactive Yellow MX-4R. The adsorbents investigated in this study were as follows: (i) bentonite intercalated by hydroxy-aluminum cations, (ii) bentonite pillared by cethyltrimethylammonium cation.

The bentonite used is original of Mostaganem city (western Algeria). Several analytical techniques were applied to identify the samples before and after treatment, such as XRD, BET, and chemical composition. The preparation of the sorbent samples was made by raw bentonite purification, followed by the intercalation step. The effects of pH medium, initial dyes concentrations, and contact time on the removal efficiency were studied. The adsorption of dyes by pillared bentonite was carried out by the isotherms construction, the fitting adsorption data by Langmuir and Freundlich equations and kinetic study.

2. Materials and methods

2.1. Materials

The bentonite used for this study was provided from M'zila deposit (Mostaganem, Algeria). This material is commercialized as Industrial Charge Bentonite (BCI) without additives by BENTAL society. Before the experiments, the samples were purified and sieved at 80 μm. The cation exchange capacity (CEC) was determined with conductimetric method [18] as 48 meq/100 g of bentonite. AlCl₃, AgNO₃, NaOH, and HCl were all of analytical grade, obtained from Aldrich.

Bemacid Yellow E 4G (C.I. acid Yellow 49) and reactive Procion Yellow MX 4R (C.I. Reactive Yellow 14) were supplied by SOITEX textile society (Tlemcen, Algeria). Synthetic test dye solutions were prepared by dissolving accurately weighed amounts of dye (1 g/L) in distilled water and subsequently diluted to required concentrations. The chemical formula and molecular weight of E-4G and MX-4R are C₁₆H₁₃Cl₂N₅O₃S; 426.24 g/mol and C₂₀H₁₉ClN₄Na₂O₁₁S₃; 669.02 g/mol, respectively. The chemical structure of the dye molecules is shown in Table 1.

2.2. Preparation of hydroxy-aluminum solution

The pillaring solution of hydroxy-aluminum cations ([Al₁₃O₄(OH)₂₄(H₂O)₁₂]⁷⁺) was prepared by adding NaOH solution (0.2 mol/L) to AlCl₃ solution (0.2 mol/L) under vigorous stirring at 60°C, until ratio molar OH[−]/Al³⁺ = 2 was reached [19]. The solution was aged at room temperature for three days before using.

2.3. Preparation of pillared bentonite

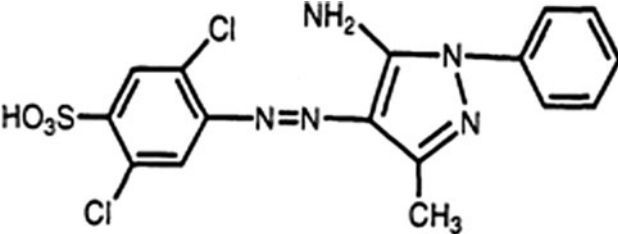
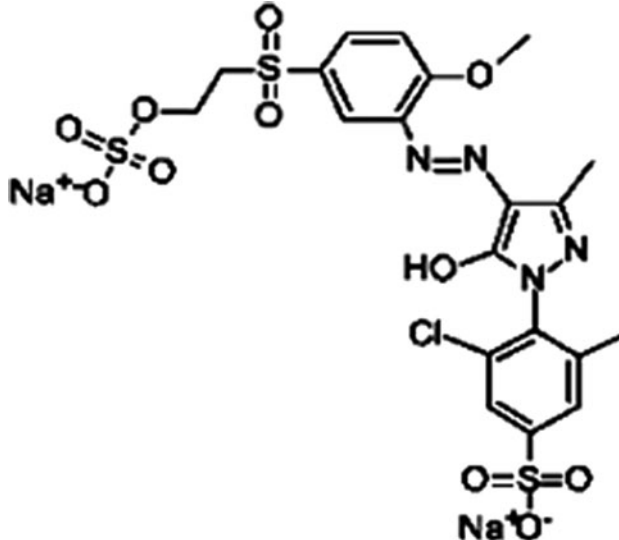
The resulting pillaring solution was added to the bentonite by stirring for 4 h at 70°C at the ratio of 50 mmol oligomeric cations per gram of bentonite [20]. The slurry was stirred for 24 h at room temperature, filtered, and washed repeatedly with deionized water until there was no chloride, verified by the AgNO₃ test. The solid was dried at 80°C and kept in a sealed bottle. The pillared bentonite obtained was designated as B-Al.

2.4. Preparation of CTAB-intercalated bentonite

Cetyltrimethylammonium bromide (CTAB) with chemical formula of C₁₉H₄₂NBr and molecular weight 364.45 g/mol was supplied by Merck, Germany.

The synthesis of CTAB-modified bentonite was performed by the following procedure: An amount of

Table 1
Chemical Structures of dyes

Bemacid Yellow E-4G	Procion Yellow MX-4R
	

1 g of bentonite was first dispersed in 100 mL of distilled water for 24 h at room temperature under vigorous agitation. Then, a desired amount of CTAB (175 mg), which is 1.0 times CEC of bentonite, was slowly added at 60°C. After 4 h of stirring, the organoclay was filtered, washed with distilled water several times, and dried at 80°C in oven. The material obtained was designated as B-CTAB.

2.5. Characterization of bentonite

The chemical analysis of natural bentonite (BN) was performed with X-fluorescence XRF 9900, Thermo instrument. X-ray analyses were performed using INEL CPS 120 diffractometer employing cobalt $K\alpha$ radiation ($\lambda = 0.178$ nm) operating at 40 kV and 25 mA with a fixed slit. The scan rate was $1.0^\circ (2\theta) \text{ min}^{-1}$, and the scan scope was from 2° to $120^\circ (2\theta)$. The specific surface area and porosity data were calculated by BET method and determined by adsorption of nitrogen via a Quantachrome instrument at -196°C . Before the adsorption tests, the samples were outgassed under vacuum over 12 h at 100°C . Residual concentrations of dyes were detected using spectrophotometer type VIS 7220 G, (Biotech Engineering Management).

2.6. Batch experimental procedure

Batch experiments were carried out by mixing 20 mL of known concentration of MX-4R and E-4G solutions with 0.1 g of B-Al or B-CTAB. The mixtures

were then agitated at room temperature ($23 \pm 1^\circ\text{C}$). The effects of contact time (10–150 min) and pH (1–7) were done for optimizing the experimental conditions. The medium pH was adjusted using 1 M HCl and 1 M NaOH. The experiments were done under agitation time of 3 h, determined from the effect of contact time experiment, after which the mixtures were filtered and the filtrates were analyzed for MX-4R and E-4G content using the spectrophotometer at wavelength of 425 and 400 nm, respectively. The amount of dye adsorbed per gram of pillared bentonite, (mg/g), was calculated as follows:

$$q_e = \frac{(C_0 - C_e)V}{m} \quad (1)$$

where C_0 and C_e are the initial and the equilibrium dye concentrations (mg/L), V is the volume of dye solution used (L), and m is the mass of material used (g).

3. Results and discussions

3.1. Characterization of raw and modified bentonite

From the elemental analysis result, the chemical composition of natural bentonite as follows: 64.22% SiO_2 , 11.62% Al_2O_3 , 9.33% CaO , 4.88% Fe_2O_3 , 3.47% MgO , 3.38% Na_2O , 1.06% TiO_2 , 0.46% SO_3 , 0.03% P_2O_5 , and 1.55% loss on ignition. The silica, alumina, and lime are the major oxides in the sample, and the

trace elements such as iron, magnesium, sodium, titanium, sulfate, and phosphor oxides are considered as impurities.

X-ray diffraction patterns of the samples are illustrated in Fig. 1. X-ray diffractogram of the BN showed a characteristic d_{001} peak of montmorillonite at $2\theta = 8.07^\circ$ ($d = 1.27$ nm) and two other peaks corresponding to the illite and the kaolinite at 2θ equal 10° and 13.75° , respectively. The hydroxy-aluminum poly-cations exchange increases the d_{001} value to 1.43 nm, but the peak was much less intense compared to that of natural bentonite, this is in agreement with previous results cited by Liang-guo et al. [21]. The reduction in diffractogram of the B-Al relative to the BN was probably due to the delamination of Mt layers by ions. The reduction in diffractogram might also be caused by collapsing of the Mt layers due to partial incongruent phase transition of hydroxy-Al into Fe/Al oxides and their interactions during aging and drying, as suggested by Thomas et al. [22].

The addition of surfactant causes the increasing of basal spacing of the bentonite around 18 Å, indicating location of CTA^+ ions between layers of montmorillonite. In order to further increase the basal spacing, CTA^+ concentration must be increased, because as known, the amount of added surfactant has a direct effect on the

interlayer expansion of Mt. The addition of CTAB in natural bentonite increases the basal spacing more than the addition of hydroxy-aluminum. These results are in agreement with previous works in the literature [23].

The BET surface area of BN was 59.02 m^2/g . After pillaring with Al_{13} and CTAB, the specific surface areas of B-Al and B-CTAB were increased to 110 and 194.4 m^2/g , respectively. The pillaring by Al_{13} showed a slight increase in the basal spacing but a significant increase in the surface area. This can be explained that in uncalcined Al-pillared clay, only electrostatic bonding exists between the negatively charged layers and the pillaring oligocations. In montmorillonites, Mg^{2+} and Fe^{3+} replace some Al^{3+} in the octahedral layer; hence, only a small quantity of these cations was exchangeable. On the other hand, the Al-pillaring process produces an important microporosity, but only a small amount of mesopores in these air-dried samples [24]. The pillaring by CTAB gives an important basal spacing and high surface area.

3.2. Effect of pH

The amounts of E-4G and MX-4R adsorbed onto pillared bentonites at various pH values are illustrated in Fig. 2. As presented in this figure, the variations of E-4G

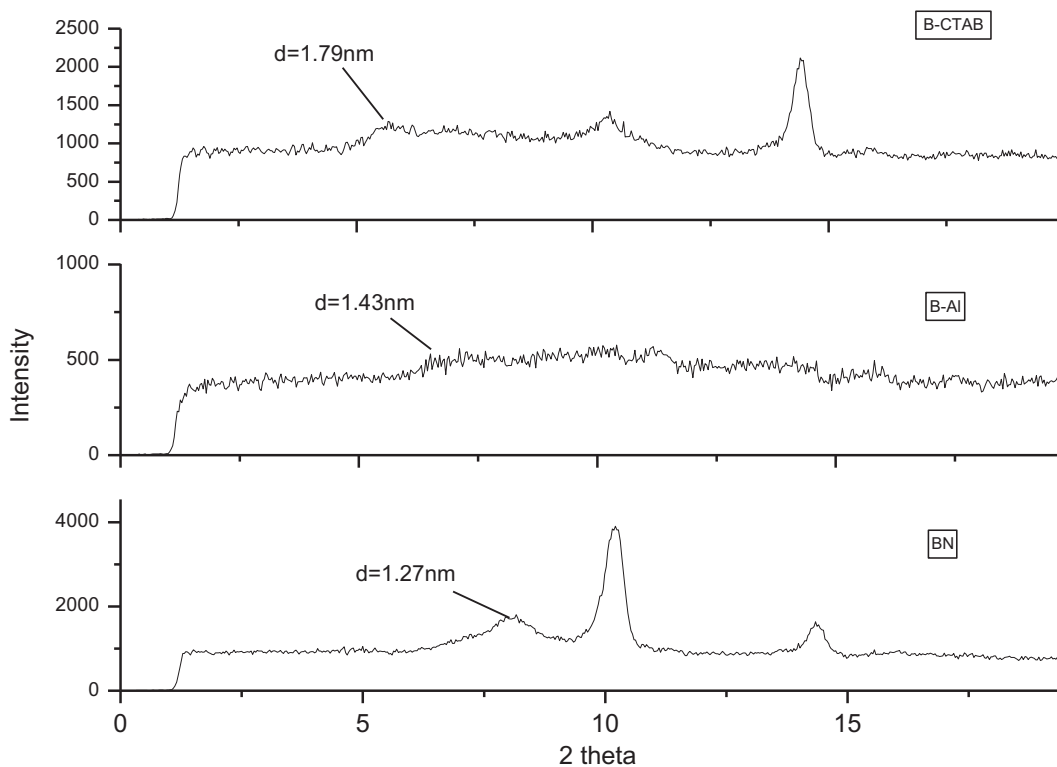


Fig. 1. XRD patterns of natural and modified bentonites.

amounts adsorbed by B-Al and B-CTAB as function of pH have the same shape, where the amounts adsorbed were high in very low pH values and decrease above pH 4. The evolution amounts adsorbed of MX-4R by two materials as function of pH are totally different. In the case of B-Al, the amount adsorbed of MX-4R increases between pH range 1 and 4, and decreases rapidly up to the pH value 6. The amount adsorbed of MX-4R by B-CTAB decreases very slowly in acid medium, then there is an inflexion point in neutral medium, where the amount adsorbed increases again to pH 8. The results confirm that the behavior of both the dyes with both the materials is totally different, but they have one thing in common that the maximum adsorption capacities of E-4G and MX-4R were noted in the acid solution, precisely in the pH range 1–4.

Since E-4G and MX-4R are anionic dyes, they are adsorbed by the samples of bentonites, which develop a positive surface charge in the acidic medium. So the best amount adsorbed of both the dyes will be at weak pH, when electric charges are of opposite sign between sorbent and adsorbate [25,26].

3.3. Adsorption isotherms

The adsorption isotherms are realized at different initial concentrations during 3 h at ambient temperature (23°C), adsorbent dose 5 g/L, and pH 2–3. The isotherms are formed by amount of dye adsorbed by the plot vs. equilibrium concentration. The adsorption isotherms of MX-4R and E-4G by the pillared bentonites are presented in Figs. 3 and 4, respectively. The results show that the amount of dye adsorbed increases with the increase in equilibrium concentration of dye. All isotherms are of S-shape according to the classification of Giles et al. [27]. The S-shape means that the adsorption is cooperative where the

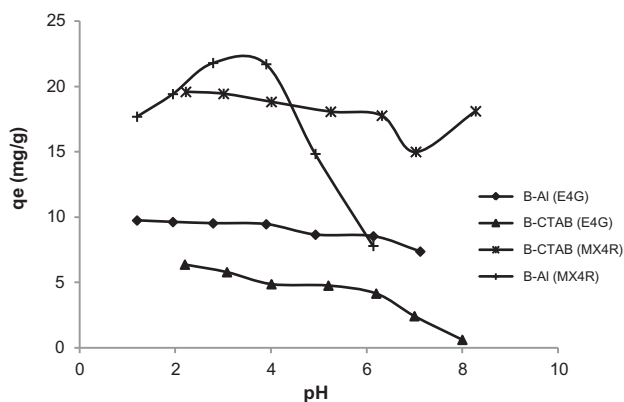


Fig. 2. Effect of pH on E-4G and MX-4R adsorptions onto pillared bentonites ($C_{0E-4G} = 50$ mg/L, $C_{0MX-4R} = 100$ mg/L, contact time 3h, adsorbent dose 5 g/L).

adsorbed molecules facilitate the adsorption of the other molecules. The amounts of MX-4R and E-4G adsorbed by B-CTAB were 93.91 and 92.75 mg/g, respectively, and these amounts adsorbed by B-Al were 66.08 and 87.72 mg/g, respectively. So the B-CTAB sample has adsorption capacity more important than B-Al for two dyes, in same operating conditions.

The Langmuir and Freundlich equations expressed in relations (2) and (3), respectively, were used for modeling the adsorption data [28,29]:

$$q_e = \frac{Q_0 K_L C_e}{1 + K_L C_e} \quad (2)$$

$$q_e = K_F C_e^{\frac{1}{n}} \quad (3)$$

where Q_0 is the maximum adsorption capacity (mg/g) and K_L (L/mg) is Langmuir adsorption constant. K_F and n are the Freundlich constants, indicating the capacity and intensity of adsorption, respectively.

Eqs. (2) and (3) can also be represented by the linear forms below:

$$\frac{C_e}{q_e} = \frac{C_e}{Q_0} + \frac{1}{K_L Q_0} \quad (4)$$

$$\log q_e = \log K_F + \frac{1}{n} \log C_e \quad (5)$$

The fitted constants for Langmuir and Freundlich models are summarized in Table 2. The regression coefficient (R^2) values obtained for Freundlich isotherm were above 0.98, indicating a very good mathematical fit by this model. The Langmuir model gives the good fit only in the case of MX-4R. The linearization constants of Langmuir equation obtained for E-4G

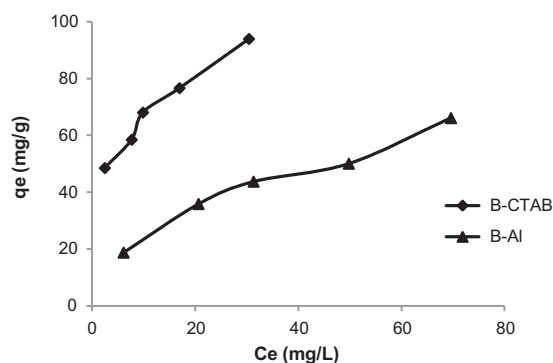


Fig. 3. Adsorption isotherms of MX-4R onto B-Al and B-CTAB ($C_{0MX-4R} = 200$ – 500 mg/L, pH = 2–3, adsorbent dose 5 g/L, contact time 3h).

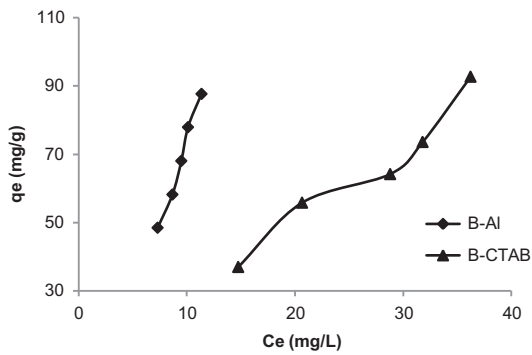


Fig. 4. Adsorption isotherms of E-4G onto B-Al and B-CTAB ($C_{0E-4G} = 200\text{--}500$ mg/L, pH = 2–3, adsorbent dose 5 g/L, contact time 3h).

dye were insignificant, and the regression correlations were very low. Similar results have been reported for the adsorption of Congo red [26] and reactive Blue 19 [30] by modified bentonite. This can be explained by the fact that the Langmuir equation is valid for monolayer adsorption onto a surface containing a finite number of identical sites, while Freundlich isotherm represents satisfactorily the sorption data on heterogeneous surfaces. The constant $1/n$ was above 1 in the case of the adsorption of E-4G by B-Al, which means the adsorption intensity was weak, but in the other cases, the $1/n$ values were lower than 1, indicating that the adsorption process is intense and favorable.

3.4. Adsorption kinetics

The adsorption kinetic data of E-4G and MX-4R were determined by testing pseudo-first-order and pseudo-second-order kinetic models. The adsorption of both the dyes on the two adsorbents increases with time and reached equilibrium at 60 min as shown in Fig. 5. The adsorption rates of the E-4G and MX-4R by intercalated bentonites are rapid early in the process and becoming slower over time. When dye concentration was low, adsorption was very fast due to the availability of the active sites and less competition.

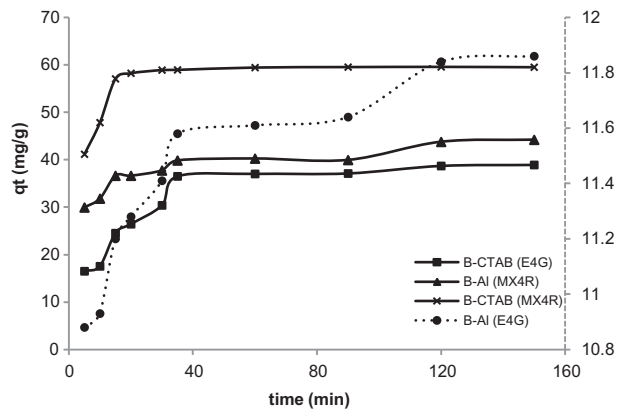


Fig. 5. Effect of contact time on E-4G and MX-4R adsorptions onto B-Al and B-CTAB ($C_{0MX-4R} = 200$ mg/L, $C_{0E-4G} = 200$ mg/L, pH = 2–3, adsorbent dose 5 g/L, contact time 3h).

With increasing dye ion concentration, competition for the adsorption sites decreased the adsorption rate [31].

The pseudo-first-order kinetic using the linear Lagergren equation is generally expressed as follows [32,33]:

$$\ln(q_e - q_t) = \ln q_e - k_1 t \quad (6)$$

where q_t is amount adsorbed of dye at time t (mg/g) and k_1 is the rate constant of the pseudo-first-order model (min^{-1}). The k_1 and q_e were calculated from the slope and intercept of plots $\ln(q_e - q_t)$ vs. t , respectively.

The pseudo-second-order kinetic is expressed as follows [34]:

$$\frac{t}{q_t} = \frac{1}{k_2 q_e^2} + \frac{t}{q_e} \quad (7)$$

where k_2 is the rate constant of the pseudo-second-order model for the adsorption process (g/mg min). Plots of t/q_t against t have been drawn to obtain the rate parameters.

Table 2
Isotherms constants

Model	Constants	Langmuir			Freundlich		
		Q_0 (mg/g)	K_L (L/mg)	R^2	$1/n$	K_F mg/g (L/mg) $^{1/n}$	R^2
B-Al	E-4G	Ins	Ins	Ins	1.396	2.96	0.984
	MX-4R	76.92	0.044	0.989	0.455	8.60	0.988
B-CTAB	E-4G	Ins	Ins	Ins	0.920	3.177	0.955
	MX-4R	113.63	0.137	0.994	0.346	28.73	0.984

Note: ins: insignificant results.

Table 3
Constant rates of the E-4G and MX-4R adsorption by B- Al and B-CTAB

Model	B-Al		B-CTAB	
	E-4G	MX-4R	E-4G	MX-4R
<i>Pseudo-first-order</i>				
$q_{e(\text{cal})}$ (mg/g)	0.835 ± 0.198	19.36 ± 1.264	35.70 ± 1.247	3.010 ± 0.762
K_1 (min^{-1})	0.019 ± 0.027	0.065 ± 0.011	0.043 ± 0.002	0.019 ± 0.009
R^2	0.809 ± 0.148	0.902 ± 0.308	0.970 ± 0.004	0.350 ± 0.080
<i>Pseudo-second-order</i>				
$q_{e(\text{cal})}$ (mg/g)	12.048 ± 0.003	45.455 ± 0.017	42.016 ± 0.022	60.24 ± 0.004
K_2 (g/mg min)	0.922 ± 0.020	0.912 ± 0.026	0.002 ± 0.0008	0.011 ± 0.005
R^2	0.999 ± 0.014	0.997 ± 0.033	0.996 ± 0.064	0.999 ± 0.001
$q_{e(\text{exp})}$ (mg/g)	11.865	44.207	38.926	59.588

The kinetic data fit the pseudo-second-order model with correlation coefficients higher than 0.98. The calculated q_e values for the dye-modified bentonite system were very close to the experimental q_e values in the case of pseudo-second-order equation, indicating that the kinetic model was appropriate. Similar studies have also been previously reported [35,36]. The pseudo-second-order model is based on the assumption that the rate-limiting step may be chemisorption which involves valence forces by sharing or electron exchange between the adsorbent and the adsorbate [37]. As can be seen from Table 3, the k_2 values of dye adsorption on B-Al (0.922 and 0.912 $\text{g mg}^{-1} \text{min}^{-1}$) were significantly greater than those of B-CTAB (0.002 and 0.011 $\text{g mg}^{-1} \text{min}^{-1}$). The maximum adsorption capacities q_e of B-CTAB calculated from pseudo-second-order model are higher than those of B-Al. This means that the adsorption of dyes onto B-Al is a fast reaction, and surfactant-modified bentonite has a best adsorption capacity due to its high porosity and its large specific surface area.

4. Conclusion

The pillared bentonites were prepared by the insertion of aluminum pillaring solution and cetyltrimethylammonium cations into the dilute bentonite suspension during 4 h. The pillared bentonites have been demonstrated to be able to adsorb E-4G and MX-4R dyes from aqueous solution.

Upon intercalation, the d_{001} spacing increased to 1.43 and 1.79 nm, for hydroxy-aluminum- and cetyltrimethylammonium-intercalated bentonite, respectively. The specific surface areas of the samples also increased from 59 m^2/g of the pure bentonite to 110 and 194.4 m^2/g of modified bentonites. All these characterization indicated the successful intercalation of bentonite. The pillared bentonites occur as good

sorbents for the removal of reactive and acid dyes at pH range of about 2–3. The adsorptions were rapid in early reactions and reached equilibrium in 60 min. The adsorption of E-4G and MX-4R dyes on pillared bentonite can be well described by pseudo-second-order. The high correlation coefficients values for the Freundlich isotherm indicate that the adsorptions occurred on a heterogeneous surface.

Nomenclature

BN	—	natural bentonite
B-Al	—	aluminum-intercalated bentonite
B-CTAB	—	cetyltrimethylammonium-intercalated bentonite
C_e	—	equilibrium concentration (mg/L)
C_0	—	initial concentration (mg/L)
E-4G	—	yellow bemacid acid dye
q_e	—	amount of dye adsorbed (mg/g)
q_t	—	amount of dye adsorbed at time t (mg/g)
Q_0	—	maximum adsorption capacity (mg/g)
k_1	—	constant rate of pseudo-first-order (min^{-1})
k_2	—	constant rate of pseudo-second-order (g/mg min)
K_L	—	Langmuir adsorption constant (L/mg)
K_F	—	Freundlich adsorption constant (mg/g(L/mg) $^{1/n}$)
m	—	mass of the adsorbent (g)
MX-4R	—	yellow procion reactive dye
V	—	volume of the solution (L)

References

- [1] N. Yener, C. Biçer, M. Önal, Y. Sarıkaya, Simultaneous determination of cation exchange capacity and surface area of acid activated bentonite powders by methylene blue sorption, *Appl. Surf. Sci.* 258 (2012) 2534–2539.
- [2] A. Tamayo, J. Kyzioł-Komosinska, M.J. Sánchez, P. Calejas, J. Rubio, M.F. Barba, Characterization and properties of treated smectites, *J. Eur. Ceram. Soc.* 32 (2012) 2831–2841.

- [3] S.A. Memon, R. Arsalan, S. Khan, T.Y. Lo, Utilization of Pakistani bentonite as partial replacement of cement in concrete, *Constr. Build. Mater.* 30 (2012) 237–242.
- [4] A. Abdel-Motilib, Z. AbdelKader, Y.A. Ragab, M. Mosalamy, Suitability of a miocene bentonite from North Western Desert of Egypt for pharmaceutical use, *Appl. Clay Sci.* 52 (2011) 140–144.
- [5] H. Liang, Z. Long, S. Yang, L. Dai, Organic modification of bentonite and its effect on rheological properties of paper coating, *Appl. Clay Sci.* 104 (2015) 106–109.
- [6] J. Guang-Peng, Y. Jian-Feng, G. Ji-Qiang, N. Koichi, Characterization of porous silicon nitride ceramics using bentonite as binder and sintering additive, *Mater. Charact.* 60 (2009) 456–460.
- [7] D.I. Stewart, P.G. Studds, T.W. Cousens, The factors controlling the engineering properties of bentonite-enhanced sand, *Appl. Clay Sci.* 23 (2003) 97–110.
- [8] G.E. Christidis, Physical and chemical properties of some bentonite deposits of Kimolos Island, Greece, *Appl. Clay Sci.* 13 (1998) 79–98.
- [9] B. Hu, H. Luo, Adsorption of hexavalent chromium onto montmorillonite modified with hydroxyaluminum and cetyltrimethylammonium bromide, *Appl. Surf. Sci.* 257 (2010) 769–775.
- [10] L.S. Belaroui, J.M.M. Millet, A. Bengueddach, Characterization of lalithe, a new bentonite-type Algerian clay, for intercalation and catalysts preparation, *Catal. Today* 89 (2004) 279–286.
- [11] H.P. Massinga Jr., W.W. Focke, L. Phillip de Vaal, M. Atanasova, Alkyl ammonium intercalation of Mozambican bentonite, *Appl. Clay Sci.* 49 (2010) 142–148.
- [12] N.R. Sanabria, P. Avila, M. Yates, S.B. Rasmussen, R. Molina, S. Moreno, Mechanical and textural properties of extruded materials manufactured with AlFe and AlCeFe pillared bentonites, *Appl. Clay Sci.* 47 (2010) 283–289.
- [13] D.C.W. Vaughan, Pillared clays: A historical perspective, *Catal. Today* 2 (1988) 187–198.
- [14] G. Lagaly, Bentonites: Adsorbents of toxic substances, *Prog. Colloid Polym. Sci.* 95 (1994) 61–72.
- [15] Q. Chen, P. Wu, Z. Dang, N. Zhu, P. Li, J. Wu, X. Wang, Iron pillared vermiculite as a heterogeneous photo-Fenton catalyst for photocatalytic degradation of azo dye reactive brilliant orange X-GN, *Sep. Purif. Technol.* 71 (2010) 315–323.
- [16] L. Zhang, L. Luo, S. Zhang, Adsorption of phenanthrene and 1,3-dinitrobenzene on cation-modified clay minerals, *Colloids Surf., A: Physicochem. Eng. Aspects* 377 (2011) 278–283.
- [17] F. Rasouli, S. Aber, D. Salari, A.R. Khataee, Optimized removal of Reactive Navy Blue SP-BR by organo-montmorillonite based adsorbents through central composite design, *Appl. Clay Sci.* 87 (2014) 228–234.
- [18] R. Navia, Environmental use of volcanic soil as natural adsorption material, PhD Thesis, University of Leoben Austria, (2004).
- [19] M.E. Roca Jalil, R. Vieira, D. Azevedo, M. Baschini, K. Sapag, Improvement in the adsorption of thiabendazole by using aluminum pillared clays, *Appl. Clay Sci.* 71 (2013) 55–63.
- [20] A. Romero-Pérez, A. Infantes-Molina, A. Jiménez-López, E.R. Jalil, K. Sapag, E. Rodríguez-Castellón, Al-pillared montmorillonite as a support for catalysts based on ruthenium sulfide in HDS reactions, *Catal. Today* 187 (2012) 88–96.
- [21] Y. Liang-guo, X. Yuan-yuan, Y. Hai-qin, X. Xiao-dong, W. Qin, D. Bin, Adsorption of phosphate from aqueous solution by hydroxy-aluminum, hydroxy-iron and hydroxy-iron-aluminum pillared bentonites, *J. Hazard. Mater.* 179 (2010) 244–250.
- [22] S.M. Thomas, J.A. Bertrand, M.L. Ocelli, F. Huggins, S.A. Gould, Microporous Montmorillonites Expanded with Alumina Clusters and $M[(\mu\text{-OH})\text{Cu}(\mu\text{-OCH}_2\text{CH}_2\text{N}(\text{Et})_2)_6(\text{ClO}_4)_3]$, ($M = \text{Al, Ga, and Fe}$), or $\text{Cr}[(\mu\text{-OCH}_3)(\mu\text{-OCH}_2\text{CH}_2\text{N}(\text{Et})_2)\text{CuCl}]_3$ Complexes, *Inorg. Chem.* 38 (1999) 2098–2105.
- [23] A. Khenifi, Z. Boubberka, K. Bentaleb, H. Hamani, Z. Derriche, Removal of 2,4-DCP from wastewater by CTAB/bentonite using one-step and two-step methods: A comparative study, *Chem. Eng. J.* 146 (2009) 345–354.
- [24] D. Tichit, F. Fajula, F. Figueras, Sintering of montmorillonites pillared by hydroxy-aluminum species, *Clays Clay Miner.* 36 (1988) 369–375.
- [25] Z. Boubberka, A. Khenifi, H. Ait Mahamed, B. Haddou, N. Belkaid, N. Bettahar, Z. Derriche, Adsorption of Supranol Yellow 4 GL from aqueous solution by surfactant-treated aluminum/chromium-intercalated bentonite, *J. Hazard. Mater.* 162 (2009) 378–385.
- [26] M. Toor, B. Jin, Adsorption characteristics, isotherm, kinetics, and diffusion of modified natural bentonite for removing diazo dye, *Chem. Eng. J.* 187 (2012) 79–88.
- [27] C.H. Giles, T.H. MacEwan, S.N. Nakhwa, D. Smith, Studies in adsorption. Part XI: A system of classification of solution adsorption isotherms, and its use in diagnosis of adsorption mechanisms and in measurements of specific surface areas of solids, *J. Chem. Soc.* 10 (1960) 3963–3973.
- [28] I. Langmuir, The adsorption of gases on plane surfaces of glass, mica and platinum, *J. Am. Chem. Soc.* 40 (1918) 1361–1403.
- [29] H.M.F. Freundlich, Über die adsorption in lösungen (About the adsorption in solutions), *Z. Phys. Chem.* 57 (1906) 385–470.
- [30] A. Özcan, Ç. Ömeröglü, Y. Erdögan, A.S. Özcan, Modification of bentonite with a cationic surfactant: An adsorption study of textile dye Reactive Blue 19, *J. Hazard. Mater.* 140 (2007) 173–179.
- [31] T.S. Anirudhan, S. Jalajamony, S.S. Sreekumari, Adsorption of heavy metal ions from aqueous solutions by amine and carboxylate functionalised bentonites, *Appl. Clay Sci.* 65–66 (2012) 67–71.
- [32] S. Lagergren, B.K. Svenska, Zur theorie der sogenannten adsorption gelöster stoffe (The theory of the adsorption of dissolved substances), *Veternskapsakad Handlingar* 4 (1898) 1–39.
- [33] Y.S. Ho, Citation review of Lagergren kinetic rate equation on adsorption reactions, *Scientometrics* 59 (2004) 171–177.

- [34] Y.S. Ho, G. McKay, The kinetics of sorption of divalent metal ions onto sphagnum moss peat, *Water Res.* 34 (2000) 735–742.
- [35] M.N. Chong, B. Jin, C.W.K. Chow, C. Saint, Recent developments in photocatalytic water treatment technology: A review, *Water Res.* 44 (2010) 2997–3027.
- [36] A. Khenifi, Z. Bouberka, F. Sekrane, M. Kameche, Z. Derriche, Adsorption study of an industrial dye by an organic clay, *Adsorption* 13 (2007) 149–158.
- [37] L. Wang, A. Wang, Adsorption properties of Congo Red from aqueous solution onto surfactant-modified montmorillonite, *J. Hazard. Mater.* 160 (2008) 173–180.